Novel Chiral Quantum Spin Liquids in Kitaev Magnets

Arnaud Ralko
Institut Néel, UPR2940, Université Grenoble Alpes et CNRS, Grenoble 38042, France

Jaime Merino
Departamento de Física Teórica de la Materia Condensada, Condensed Matter Physics Center (IFIMAC) and Instituto Nicolás Cabrera, Universidad Autónoma de Madrid, Madrid 28049, Spain

(Received 24 October 2019; accepted 13 May 2020; published 26 May 2020)

Quantum magnets with pure Kitaev spin exchange interactions can host a gapped quantum spin liquid with a single Majorana edge mode propagating in the counterclockwise direction when a small positive magnetic field is applied. Here, we show how under a sufficiently strong positive magnetic field a topological transition into a gapped quantum spin liquid with two Majorana edge modes propagating in the clockwise direction occurs. The Dzyaloshinskii-Moriya interaction is found to turn the nonchiral Kitaev's gapless quantum spin liquid into a chiral one with equal Berry phases at the two Dirac points. Thermal Hall conductance experiments can provide evidence of the novel topologically gapped quantum spin liquid states predicted.

DOI: 10.1103/PhysRevLett.124.217203

A quantum spin liquid (QSL) is an exotic state of matter in which localized spins do not order even at zero temperature in contrast to magnetic ordering observed in conventional insulating magnets. QSLs are highly entangled states which cannot be characterized by a Landau local order parameter. Exhibiting topological order, emergent gauge fields and fractional excitations [1,2], they are at the heart of an intense research activity. The first concrete example of a two-dimensional QSL has been the resonating valence bond (RVB) state envisioned by Anderson [3] to describe the ground state of triangular antiferromagnets and as the parent insulating phase of high-T_c superconductors. Due to the spin correlations, a spin-flip in an RVB state fractionalizes into two neutral spin-1/2 particles (spinons) which can propagate freely around the lattice. In spite of intense experimental efforts, there is no unambiguous observation of fractionalization—such as the expected spinon continuum in the spin excitation spectra—in real materials.

The interplay between strong Coulomb interaction and spin-orbit coupling [4] in the honeycomb magnets such as A_2IrO_3 [5] (with $A = $ Li, Na), $H_3LiIr_2O_6$ [6], α-$RuCl_3$, and organometallic frameworks [7] can lead to special compass interactions which frustrate the magnetic order of the $S = 1/2$ pseudospins. The exact QSL ground sate of the Kitaev [8] model has opened the possibility of finding fractionalized excitations in spin-orbit coupled Mott insulators on honeycomb lattices. From the decomposition of the spin operators onto four noninteracting Majorana fermions, Kitaev showed that the elementary spin excitations of the Kitaev QSL (KQSL) are fractionalized into itinerant Majorana fermions with Dirac dispersion, and localized ones giving Z_2 gauge fluxes. Recent observations on α-$RuCl_3$ [9,10] and $H_3LiIr_2O_6$ [6] have been interpreted in terms of the existence of such two types of excitations.

However, a realistic description of honeycomb materials requires including additional spin interactions not included in the Kitaev model as well as considering large magnetic fields beyond the perturbative regime discussed so far. Since there is no exact solution in these physically relevant situations new theoretical approaches are required to properly describe the system. For instance, exact numerical and slave fermion approaches [11–13] of the Kitaev model have found a transition to a gapless U(1) spin liquid phase under sufficiently strong applied magnetic fields [14,15]. On the other hand, the effect of Heisenberg and symmetric spin exchange terms needs to be considered [16,17] in order to accurately describe the magnetically ordered phases [18] observed in Na_2IrO_3 and α-$RuCl_3$. Finally, the next-nearest-neighbor Dzyaloshinskii-Moriya (DM) has been invoked as being relevant for the description of real materials [19] but its effect on the Kitaev model remains little explored so far [20].

Here, we report on two novel topological QSLs arising when either a strong magnetic field or a DM interaction are considered in the pure Kitaev model. We have discovered that the gapped QSL state with Chern number $\nu = \pm 1$ (depending on the direction of the field) predicted at low tilted magnetic fields [8], undergoes a novel topological transition to a different, topologically gapped QSL with $\nu = \pm 2$. Such topological transition occurs in a regime in which the Dirac cones disappear due to strong hybridization between itinerant and localized Majorana fermions. We also predict the presence of a novel gapless chiral QSL induced by the DM interaction and that is characterized by

equal Berry phases at the two Dirac cones ($\phi_K = \phi_{K'} = \pm\pi$) in contrast to the opposite Berry phases found in the pure Kitaev model ($\phi_K = -\phi_{K'} = \pm\pi$). The novel topological gapped QSL states found here could be tested through thermal Hall experiments.

Since we are interested in the description of competing topological phases starting from the KQSL, the $H_K = 2\sum_{\langle ij\rangle,\gamma} K^\gamma S_i^\gamma S_j^\gamma$—where the three nearest-neighbor bonds $\langle ij\rangle$ of the honeycomb lattice are denoted by $\gamma = x, y, z$—is the most relevant starting point [21]. We emphasize the factor of 2 in the definition of the model. The next-nearest-neighbor DM interaction: $H_{\mathrm{DM}} = \sum_{\langle\langle ij\rangle\rangle} \mathbf{D}_{ij} \cdot \mathbf{S}_i \times \mathbf{S}_j$ is also important for describing the magnetic orders observed in Iridates [19,28], and it is known that, combined with the magnetic field, can open a nontrivial topological gap. For this purpose, we also consider the term $H_B = -\sum_i \mathbf{B} \cdot \mathbf{S}_i$. Hence, the final Hamiltonian reads:

$$H = H_K + H_{\mathrm{DM}} + H_B, \tag{1}$$

and we will consider an isotropic Kitaev interaction, i.e., $K^\gamma = K$ in the rest of the Letter, as well as a the magnetic field $\mathbf{B}$ and the DM interaction $\mathbf{D}_{ij} = \mathbf{D}$ parametrized in function of tilt parameters t and d as $\mathbf{B} = B(t, t, 1)/\sqrt{1+2t^2}$ and $\mathbf{D} = D(d, d, 1)/\sqrt{1+2d^2}$, respectively, both ranging from the pure z direction (t or $d = 0$) to the case perpendicular to the honeycomb plane (t or $d = 1$).

The full model is treated using Kitaev's Majorana decomposition of the spin $S^\alpha = \frac{1}{4}(ib^\alpha c - i\frac{1}{2}\epsilon_{\alpha,\beta,\delta} b^\beta b^\delta)$ [8] where greek letters span the space dimensions (x, y, z) and $\epsilon_{\alpha,\beta,\delta}$ is the Levi-Civita symbol (Fig. 1). In this notation, b operators correspond to flux band variables while c describes the itinerant Majorana fermions. These are in the presence of the three other localized Majoranas which act as gauge fluxes [see Fig. 3(a) for the dispersion relation of the pure Kitaev model].

Going away from the specific Kitaev point requires the proper consideration of the constraint on the number of fermions—four Majoranas per spin—that can be only achieved in average by introducing Lagrange multipliers $\{\lambda_i\}$:

$$H_L = \frac{i}{4}\sum_{i,\alpha}\lambda_\alpha\left[b_i^\alpha c_i + \frac{1}{2}\epsilon_{\alpha\beta\delta} b_i^\beta b_i^\delta\right],$$

where summation over repeated indices is assumed. The explicit implementation of the fermion constraint is crucial for a proper description of model (1) containing terms other than the pure Kitaev contribution and we have provided all details in [22].

The complete phase diagram of model (1) can be nicely represented in a ternary plot as displayed in Fig. 1 for $\mathbf{B}$ in the [1,1,1] direction ($t = 1$) and $\mathbf{D}$ along the z direction

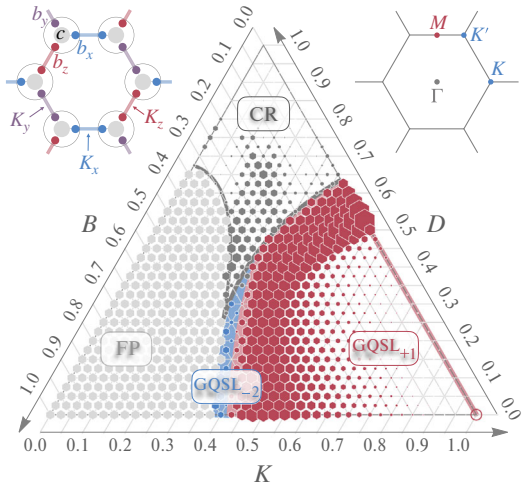

FIG. 1. Phase diagram of Kitaev model with DM interaction under magnetic field. The full phase diagram of the Kitaev model in the presence of a magnetic field pointing in the [1,1,1] direction ($t = 1$) is shown. Empty regions indicate gapless phases and the size of the hexagonal symbols indicate the size of the gap. Gray areas correspond to the gapped fully polarized (FP) phase with Chern number $\nu = 0$, the red to a gapped QSL with $\nu = +1$ denoted as GQSL$_{+1}$. A gapped QSL with an unconventional Chern number of $\nu = -2$, termed GQSL$_{-2}$ (dark blue) occurs between the FP and the GQSL$_{+1}$. Away the KQSL at $K = 1$ (open circle), an ungapped QSL, UQSL (thick red line) with equal Berry phases at the two Dirac points occurs for $B = 0$ and $K = 1$ at a nonzero DM, $D < 0.5$, which becomes the GQSL$_{+1}$ around $D \sim 0.5$–0.65, to finally become gapless and nontopological at a larger D (dark gray). In this region, CR refers to classical regimes, beyond the accessibility of the present theory. The left inset shows the Majorana decomposition of the model considered while the right inset shows the first Brillouin zone and symmetry points of the honeycomb lattice.

($d = 0$) for simplicity, realizing that the case $d = 1$ is qualitatively similar. On this graph only, the full parameter range of the model onto the plane fulfills the constraint $K + D + B = 1$, providing $K > 0$, $D > 0$ and $B > 0$, the area of the hexagons is proportional to the gap at this point, and the color refers to different states of matter. In this (K, D, B) constrained space, the vertex defined by (0,0,1) corresponds to the topologically trivial ($\nu = 0$) fully polarized (FP) state, (1,0,0), to the gapless Kitaev QSL (KQSL) and (0,1,0) to a gapless classical state whose magnetic properties remain yet to be determined. Three different topological phases characterized by their Chern numbers can be distinguished in the phase diagram. A gapped topological QSL with $\nu = +1$ denoted by GQSL$_{+1}$ is topologically equivalent to the QSL found by Kitaev at weak magnetic fields. The novel gapped QSL with unconventional Chern number of $\nu = -2$ is denoted by GQSL$_{-2}$. The gray areas correspond to the FP state with $\nu = 0$. The mechanisms driving these topological states are explained below, but we emphasize here the presence of the two novel gapped topological QSL with large Chern numbers,

$\nu = \pm 2$. These are the result of the strong competition between the three terms entering the hamiltonian and occur in intermediate regions between the FP and the GQSL_{+1} phases. These phases are *chiral* QSLs since time reversal symmetry is broken either explicitly by the applied magnetic field or spontaneously for $B = 0$ and $D \neq 0$. Interestingly, at zero field, $B = 0$, a small but finite DM of $D \lesssim 0.5$ (with $K = 1$) leads to equal Berry phases, ϕ_k, around the Dirac nodes (see Fig. 1 for the first Brillouin zone of the lattice) $\phi_K = \phi_{K'} = \pm\pi$ in contrast to the opposite Berry phases found in the pure Kitaev model, $\phi_K = -\phi_{K'} = \pm\pi$. Hence, we have unraveled a new ungapped QSL with nonzero chirality which we denote by UQSL.

Applying a tilted magnetic field is found to open a gap in the Majorana fermion spectrum, consistent with perturbation theory [8]. The gap is opened symmetrically with respect to the zero energy and the resulting gapped QSL is topological with a nonzero Chern number $\nu = \pm 1$, the sign depending on the direction of the magnetic field. Our gap arises naturally from imposing the constraints on the Majorana fermions in contrast to a previous Majorana mean field analysis which add by hand a three-spin term to be able to open a gap [29]. We associate the gap opening to the nonzero Lagrange multipliers (2) which lead to local hybridization between matter and flux Majorana fermions for $B \neq 0$. We note that the one-particle constraints are not automatically verified when considering models beyond the pure Kitaev model even at the mean-field level so it is necessary to impose them explicitly [22]. Hence, our MMFT is capable of describing correctly the exact KQSL at $B = 0$ as well as the gapped QSL under low magnetic fields without making any extra assumptions. We finally note that closely related Abrikosov fermion mean-field theories [18] imposing the one single-particle constraint through a single Lagrange multiplier [30] (our λ_z) instead of three [31]—as we have done—can lead to different results to our MMFT [22].

Concomitantly with the gap opening, the magnetic field leads to nonzero chiral currents of Majorana fermions between the next nearest neighbor (NNN) sites as shown in Fig. 2(a). Only when the three components of the magnetic field are nonzero, all λ_α are simultaneously nonzero as well. This leads to hybridization among the four Majoranas at each site which ultimately leads to the gap opening. The size of the gap depends on t, the actual orientation of the magnetic field. When the field is parallel to one of the natural axis (say $t = 0$ for $\mathbf{B} = Bu_z$), the gap is zero and we have a gapless QSL. At a critical B we find that the $\pm\pi$ Berry phases at the Dirac points can switch their signs as found earlier [29].

We now discuss the effect of DM on the pure Kitaev model ($B = 0$). As stated above, as the DM is increased the Berry phases around the Dirac points become equal: $\phi_K = \phi_{K'} = \pm\pi$, indicating a change in the nature of the KQSL which characterizes the UQSL. As the D parameter is further increased above a critical value, $D \gtrsim 0.5$ (with $B = 0$ and $K = 1$), the system opens up a gap leading to a topologically gapped *chiral* QSL with $\nu = \pm 1$ for either $d = 0$ or 1, $\mathrm{GQSL}_{\pm 1}$. The origin of the nonzero Chern number may be associated with the occurrence of *anisotropic* chiral amplitudes between NNN sites as shown in Fig. 2(b) for $d < 1$. This lattice nematicity induced by anisotropy of $\mathbf{D}$ is completely restored for $d = 1$ at which the NNN chiral amplitudes are the ones displayed in (a). In any case, the DM interaction induces both an *ungapped* and a *gapped* phase. This UQSL is a novel QSL which breaks time reversal symmetry spontaneously in contrast with the *gapped* chiral QSL reported on the decorated honeycomb lattice [32] due to its gapless character. When a [001] magnetic field ($t = 0$) is applied in the presence of a nonzero DM, a gapless QSL with the two Dirac cones shifted in opposite directions by the same amount occurs. The sublattice symmetry respected by the DM interaction protects Dirac cones from opening a gap. By tilting the magnetic field to $t = 1$, a gap opens up as found in the case of zero DM leading to a $\mathrm{GQSL}_{\pm 1}$. But unlike opening symmetrically around zero, the gap centers are equally shifted in opposite directions at the two cones. In Fig. 3 we show the evolution of the Majorana dispersions under a [111] magnetic field ($t = 1$). With no magnetic field applied the MMFT dispersions consist on gapless Majorana matter bands touching at the Dirac points and flat bands describing localized Z_2 fluxes. The flat bands are threefold degenerate in this case. As the magnetic field increases up to about $B \sim 0.6$, (with $K = 1$) a gap opens up at the Dirac points while the flux bands remain almost flat.

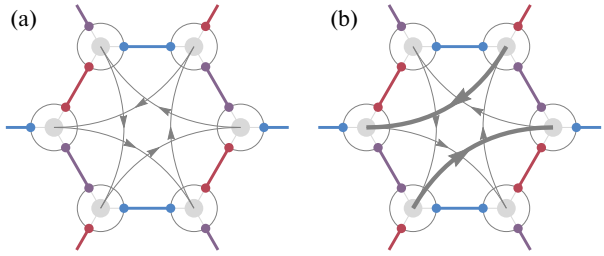

FIG. 2. Chiral amplitudes in the Kitaev model from the Majorana mean-field theory. In (a) we show the NNN chiral Majorana amplitudes, $\langle c_i c_j \rangle$, induced in the ground state MMFT wave function either by a magnetic field perpendicular to the plane, $t = 1$, or a DM vector oriented perpendicular to the plane ($d = 1$). These are responsible for the *chiral* QSL with Chern number $\nu = +1$ (GQSL_{+1}) discussed in the text. (b) Anisotropic amplitudes (the thickness corresponds to the different strength) arising from finite DM $d \neq 1$ (with no applied magnetic field) responsible for the opening of the gap for $0.5 < D < 0.65$ (with $K = 1$ and $d = 0$) in the GQSL_{+1}. The snapshots show one of the two possible chiralities of the ground state ($\nu = +1$). Note that (a) and (b) amplitudes are smoothly connected as shown in the phase diagram of Fig. 1.

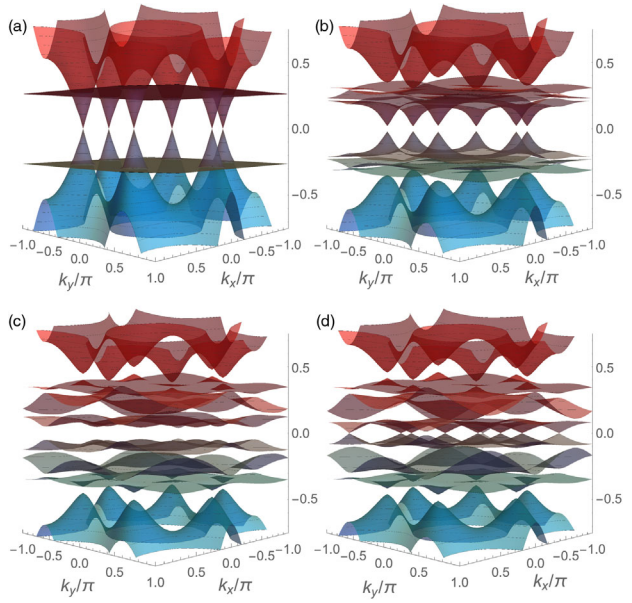

FIG. 3. Majorana dispersions of the Kitaev model under a tilted external magnetic field and zero DM interaction. The evolution of the Majorana dispersions under a tilted $t = 1$ magnetic field comparing the case (a) with no applied magnetic field, $B = 0$, consisting of gapless Majorana dispersions and flat flux bands (threefold degenerate) describing the Z_2 fluxes, (b) with $B \simeq 0.6$, where a gap has already opened and the flux Majorana bands remain flat. This gapped QSL with Chern number $\nu = +1$, GQSL_{+1}, persists up to $B_c = 1.43$ is adiabatically connected with the KQSL, (c) with $B = 1.2$, the Dirac cones have been washed out and the gapped fluxes are strongly distorted becoming dispersive, (d) with $B = 1.43$, a gapped QSL with $\nu = -2$, GQSL_{-2}, arises between B_c and $B \simeq 1.64$ indicating a different topological state from the KQSL. $K \equiv 1$ in this plot.

This GQSL_{+1} phase—since it is gapped and $\nu = +1$—is adiabatically connected to the gapped QSL found by Kitaev [8]. As the magnetic field is increased up to $B_c \simeq 1.43$ the flux bands are gradually distorted becoming dispersive and strongly hybridized with the Majorana matter bands. Note also how the bands are becoming closer at the three M points for $B \sim B_c$. As the field is increased beyond B_c, a gap opens up at this newly formed band touching M points with Berry flux magnitudes larger than π in contrast to typical Dirac cones. This can be attributed to the fact that the matter and flux Majoranas are now forming unseparable composite objects due to the strong hybridization in this magnetic field regime [22]. Hence, we find a gapped topological QSL with Chern number $\nu = -2$ emerging in the range $B \in [1.43, 1.64]$. It is interesting to note that a CSL with $\nu = 2$ has been found in [30] but with an extra symmetric spin term in the Hamiltonian. At larger magnetic fields ($B > 1.64$) there is a transition to a gapped and fully polarized insulator with a trivial topology ($\nu = 0$)—the full polarization is an artifact of the method. The Majorana dispersions are also strongly modified by D even for $B = 0$. Recent numerical studies [11–22,28–33] suggest the existence of a *gapless* intermediate phase in a somewhat similar parameter range. In spite of the different features found (gapless vs gapped), our gap closing around B_c can be associated with the large enhancement of low energy excitations developing near the PL phase. Interestingly, we have supported by ED the fact that D and B combined possibly lead to a gap opening. All these points are detailed in [22].

To conclude, we discuss our results in the context of Kitaev materials. Although they are mostly believed to have ferromagnetic couplings [4,19,34], some works suggest [35,36] AFM couplings as mostly considered here. QSL behavior has recently been observed in the honeycomb magnet $H_3LiIr_2O_6$ [6] with the caution that H disorder in this material can deviate magnetic couplings from the Kitaev model [37,38]. Although α-$RuCl_3$ is magnetically ordered, there is experimental evidence for its proximity to a QSL phase [36,39]. Under high pressure above 1 GPa [40] or applying a magnetic field destroys AF order giving way to a gapped QSL [41,42]. Strikingly, recent thermal Hall conductivity experiments find fractional quantization of the thermal conductance which is attributed to the Majorana edge modes in a GQSL_{+1} [9]. Nuclear magnetic resonance experiments find a spin gap $\Delta \propto B^3$ at small fields [10] due to the fractionalization of the spin into two gauge fluxes and a gapped Majorana fermion as predicted by Kitaev [8]. Figure 4 shows that a similar spin gap opening with a [111] magnetic field and zero DM should be observed in antiferromagnetic (AFM) Kitaev materials. Figure 4 also shows that in AFM Kitaev materials, the

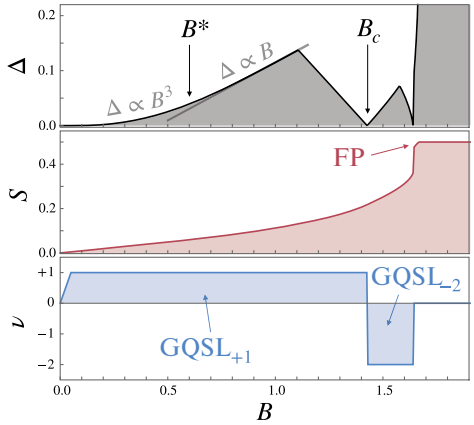

FIG. 4. Dependence of the gap (top), the magnetic moment (middle) and the Chern number (bottom) with an applied magnetic field and zero DM interaction. The gap obtained from the MMFT changes from $\Delta \propto B^3$, expected from perturbation theory, to $\Delta \propto B$ around $B^* \sim 0.6$ under the magnetic field $\mathbf{B} = B(1,1,1)/\sqrt{3}$. A topological transition from a gapped QSL with Chern number, $\nu = +1$, GQSL_{+1}, to a QSL with $\nu = -2$, GQSL_{-2}, occurs at $B_c \sim 1.43$. For $B \gtrsim 1.64$ a topologically trivial polarized insulator is stabilized. $K = 1$ in this plot.

$GQSL_{+1}$ (under a positive magnetic field) would survive up to an applied tilted magnetic field of $B \lesssim B_c$, way beyond the perturbative regime. The Majorana edge states in this QSL will contribute to the thermal Hall conductance [8,43], $\kappa_{xy}/T = (\pi/12)(k_B^2/\hbar d)$, as recently observed [9]. This is half and opposite in sign to the thermal Hall conductance observed in an integer quantum Hall effect experiment [44] associated with electronic charge. Strikingly, since a distinct gapped QSL with $\nu = -2$ in the range $B \sim 1.43$–1.64 arises ($\sim$90 Tesla using $2K \approx 7$ meV for α-$RuCl_3$), our analysis predicts a sudden jump of κ_{xy}/T, the thermal Hall coefficient, from $(\pi/12)(k_B^2/\hbar d)$ to $-(\pi/6)(k_B^2/\hbar d)$ around B_c. This signals a novel topological transition in AFM Kitaev magnets that could be searched experimentally.

J. M. acknowledges financial support from (Grant No. RTI2018-098452-B-I00) MINECO/FEDER, Unión Europea, from the María de Maeztu Programme for Units of Excellence in R&D (Grant No. CEX2018-000805-M), from (mobility program: "Salvador de Madariaga": Grant No. PRX18/00070) Ministerio de Educación, Cultura y deporte in Spain and the hospitality from Néel Institute in Grenoble. We thank the anonymous referee for pointing out that the gap closing to the fully polarized state was overlooked in the first version.

[1] L. Balents, Spin liquids in frustrated magnets, Nature (London) **464**, 199 (2010).
[2] L. Savary and L. Balents, Quantum spin liquids: A review, Rep. Prog. Phys. **80**, 016502 (2017).
[3] P. W. Anderson, Resonating valence bonds: A new kind of insulator?, Mater. Res. Bull. **8**, 153 (1973).
[4] G. Jackeli and G. Khalliulin, Mott Insulators in the Strong Spin-Orbit Coupling Limit: From Heisenberg to a Quantum Compass and Kitaev Models, Phys. Rev. Lett. **102**, 017205 (2009).
[5] H. Takagi, T. Takayama, G. Jackeli, and G. Khaliullin, Kitaev quantum spin liquid-concept and materialization, Nat. Rev. Phys. **1**, 264 (2019).
[6] K. Kitagawa, T. Takayama, Y. Matsumoto, A. Kato, R. Takano, Y. Kishimoto, S. Bette, R. Dinnebier, G. Jackeli, and H. Takagi, A spin-orbital entangled quantum liquid on honeycomb lattice, Nature (London) **554**, 341 (2018).
[7] M. G. Yamada, H. Fujita, and M. Oshikawa, Designing Kitaev Spin Liquids in Metal-Organic Frameworks, Phys. Rev. Lett. **119**, 057202 (2017).
[8] A. Kitaev, Anyons in an exactly solvable model and beyond, Ann. Phys. (Amsterdam) **321**, 2 (2006).
[9] Y. Kasahara *et al.*, Majorana quantization and half-integer thermal quantum Hall effect in a Kitaev spin liquid, Nature (London) **559**, 227 (2018).
[10] N. Jansa, A. Zorko, M. Gomilšek, M. Pregelj, K. W. Krämer, D. Biner, A. Biffin, C. Rüegg, and M. Klanjšek, Observation of two types of fractional excitation in the Kitaev honeycomb magnet, Nat. Phys. **14**, 786 (2018).
[11] Y. F. Jiang, T. P. Devereaux, and H.-C. Jiang, Field-induced quantum spin liquid in the Kiatev-Heisenberg model and its relation to α-$RuCl_3$, Phys. Rev. B **100**, 165123 (2019).
[12] H.-C. Jiang, C.-Y. Wang, B. Huang, and Y.-M. Lu, Field induced quantum spin liquid with spinon Fermi surfaces in the Kitaev model, arXiv:1809.08247v2.
[13] L. Zou and Y.-C. He, Field-induced neutral Fermi surface and QCD_3-Chern-Simons quantum criticalities in Kitaev materials, Phys. Rev. Research **2**, 013072 (2020).
[14] C. Kickey and S. Trebst, Emergence of a field-driven U(1) spin liquid in the Kitaev honeycomb model, Nat. Commun. **10**, 1038 (2019).
[15] Z. Zhu, I. Kimchi, D. N. Sheng, and L. Fu, Robust non-Abelian spin liquid and a possible intermediate phase in the antiferromagnetic Kitaev model with magnetic field, Phys. Rev. B **97**, 241110(R) (2018).
[16] R. Schaffer, S. Bhattacharjee, and Y. B. Kim, Quantum phase transition in Heisenberg-Kitaev model, Phys. Rev. B **86**, 224417 (2012).
[17] J. Knolle, S. Bhattacharjee, and R. Moessner, Dynamics of a quantum spin liquid beyond integrability: The Kiatev-Heisenberg-Γ model in an augmented parton mean-field theory, Phys. Rev. B **97**, 134432 (2018).
[18] M. Gohlke, G. Wachtel, Y. Yamaji, F. Pollmann, and Y. B. Kim, Quantum spin liquid signatures in Kitaev-like frustrated magnets, Phys. Rev. B **97**, 075126 (2018).
[19] S. M. Winter, Y. Li, H. O. Jeschke, and R. Valentí, Challenges in design of Kitaev materials: Magnetic interactions from competing energy scales, Phys. Rev. B **93**, 214431 (2016).
[20] A. V. Lunkin, K. S. Tikhonov, and M. V. Feigel'man, Perturbed Kitaev model: Excitation spectrum and long-ranged spin correlations, J. Phys. Chem. Solids **128**, 130 (2019).
[21] We have mapped out the phase diagram of the Heisenberg-Kitaev model confirming the presence of an extended KQSL phase (see the Supplemental Material Ref. [22]). Without loss of generality, we can thus restrict our study to the pure Kitaev case.
[22] See Supplemental Material at http://link.aps.org/supplemental/10.1103/PhysRevLett.124.217203 for (i) details of the Majorana mean field theory, (ii) the extension to the Heisenberg-Kitaev model, (iii) the effect of the DM interaction on the Majorana spectrum, (iv) the computation of the multiband Berry phases and Chern numbers, and (v) the effect of the single-occupancy constraint on magnetic properties of the model. It includes Refs. [23–27].
[23] J. Dennis and J. Moré, Quasi-Newton methods motivation and theory, SIAM Rev. Soc. Ind. Appl. Math. **19**, 46 (1977).
[24] J. Chaloupka, G. Jackeli, and G. Khaliullin, Kitaev-Heisenberg Model on a Honeycomb Lattice: Possible Exotic Phases in Iridium Oxides A_2IrO_3, Phys. Rev. Lett. **105**, 027204 (2010).
[25] H.-C. Jiang, Z.-C. Gu, X.-L. Qi, and S. Trebst, Possible proximity of the Mott insulating iridate Na_2IrO_3 to a topological phase: Phase diagram of the Heisenberg-Kitaev model in a magnetic field, Phys. Rev. B **83**, 245104 (2011).
[26] D. Gotfryd, J. Rusnačko, K. Wohlfeld, G. Jackeli, J. Chaloupka, and A. M. Oleś, Phase diagram and spin correlations of the Kitaev-Heisenberg model: Importance of quantum effects, Phys. Rev. B **95**, 024426 (2017).

[27] T. Fukui, Y. Hatsugai, and H. Suzuki, Chern numbers and discretized Brillouin zone: Efficient method of computing (spin) Hall conductances, J. Phys. Soc. Jpn. **74**, 1674 (2005).
[28] N. B. Perkins, Y. Sizyuk, and P. Wölfle, Interplay of many-body and single-particle interactions in iridates and rhodates, Phys. Rev. B **89**, 035143 (2014).
[29] J. Nasu, Y. Kato, Y. Kamiya, and Y. Motome, Succesive Majorana topological transitions driven by a magnetic field in the Kitaev model, Phys. Rev. B **98**, 060416(R) (2018).
[30] Z.-X. Liu and B. Normand, Dirac and Chiral Quantum Spin Liquids on the Honeycomb Lattice in a Magnetic Field, Phys. Rev. Lett. **120**, 187201 (2018).
[31] W. Choi, P. W. Klein, A. Rosch, and Y. B. Kim, Topological superconductivity in the Kondo-Kitaev model, Phys. Rev. B **98**, 155123 (2018).
[32] H. Yao and S. A. Kivelson, Exact Chiral Spin Liquid with Non-Abelian Anyons, Phys. Rev. Lett. **99**, 247203 (2007).
[33] S. Pradhan, N. D. Patel, and N. Trivedi, Two-magnon bound states in the Kitaev model in a [111]-field, Phys. Rev. B **101**, 180401 (2020).
[34] S. M. Winter, A. A. Tsirlin, M. Daghofer, J. van den Brink, Y. Singh, P. Gegenwart, and R. Valentí, Models and materials for generalized Kitaev magnetism, J. Phys. Condens. Matter **29**, 493002 (2017).
[35] H.-S. Kim, V. Shankar, A. Catuneanu, and H.-Y. Kee, Kitaev magnetism in honeycomb RuCl3 with intermediate spin-orbit coupling, Phys. Rev. B **91**, 241110(R) (2015).
[36] A. Banerjee, J. Yan, J. Knolle, C. A. Bridges, M. B. Stone, M. D. Lumsden, D. G. Mandrus, D. A. Tennant, R. Moessner, and S. E. Nagler, Neutron scattering in the proximate quantum spin liquid α-$RuCl_3$, Science **356**, 1055 (2017).
[37] Y. Li, S. M. Winter, and R. Valentí, Role of Hydrogen in the Spin-Orbital-Entangled Quantum Liquid Candidate $H_3LiIr_2O_6$, Phys. Rev. Lett. **121**, 247202 (2018).
[38] R. Yadav, R. Ray, M. S. Eldeeb, S. Nishimoto, L. Hozoi, and J. van den Brink, Strong Effect of Hydrogen Order on Magnetic Kitaev Interactions in $H_3LiIr_2O_6$, Phys. Rev. Lett. **121**, 197203 (2018).
[39] A. Banerjee *et al.*, Proximate Kitaev quantum spin liquid behaviour in a honeycomb magnet, Nat. Mater. **15**, 733 (2016).
[40] Z. Wang *et al.*, Pressure-induced melting of magnetic order and emergence of a new quantum state in α-$RuCl_3$, Phys. Rev. B **97**, 245149 (2018).
[41] R. Hentrich *et al.*, Unusual Phonon Heat Transport in α-$RuCl_3$: Strong Spin-Phonon Scattering and Field-Induced Spin Gap, Phys. Rev. Lett. **120**, 117204 (2018).
[42] S.-H. Baek, S.-H. Do, K.-Y. Choi, Y. S. Kwon, A. U. B. Wolter, S. Nishimoto, J. van den Brink, and B. Büchner, Evidence for a Field-Induced Quantum Spin Liquid in α-$RuCl_3$, Phys. Rev. Lett. **119**, 037201 (2017).
[43] K. Nomura, S. Ryu, A. Furusaki, and N. Nagaosa, Cross-Correlated Responses of Topological Superconductors and Superfluids, Phys. Rev. Lett. **108**, 026802 (2012).
[44] C. L. Kane and M. P. A. Fisher, Quantized thermal transport in the fractional quantum Hall effect, Phys. Rev. B **55**, 15832 (1997).